Stanford Exploration Project, Report 82, May 11, 2001, pages 1–88

Prestack migration velocity analysis using wavefront synthesis

Jun Ji [1]

ABSTRACT

Common-reflection-point (CRP) gathers provide important clues in various migration velocity analysis schemes (Al-Yahya, 1987; Etgen, 1990). Conventionally, CRP gathers are obtained by prestack migration of shot records or constant-offset sections. This paper introduces a way to generate a CRP gather for residual velocity analysis using wavefront synthesis imaging. Compared to CRP gathers obtained by other prestack migrations, those obtained by wavefront synthesis imaging provide a better resolution residual velocity panel. As a result, we can easily determine and get more reliable residual velocity, which is very important in inverting it into the true interval velocity of a medium.

INTRODUCTION

In a multifold seismic experiment, a small portion of the subsurface is illuminated by shots at different offsets. The reflected energy is recorded by a receiver on the surface. Imaging of such seismic reflection data can be accomplished by prestack depth migration of individual shot records or constant-offset sections, followed by a stacking of the results at common reflection locations. When the correct velocity model is used to depth-migrate a dataset before stacking, the images of a reflector on the migrated constant-offset sections are located at identical positions. If the velocity model is inaccurate, the images of a reflector will have residual moveout over offset. In this case, stacking of the common-reflection-point (CRP) gathers cannot effectively enhance the signal-noise ratio of the images. It may even degrade the images. After profile migration, the moveout trajectories on CRP gathers can curve upward or downward, depending on whether the migration velocities are higher or lower than the true velocities. Using this property, Al-Yahya (1987) employed profile migration for velocity analysis. In his method, velocity errors are estimated by measuring the curvatures of the residual moveout in CRP gathers. Al-Yahya's curvature scanning is based on the residual moveout equation with common-midpoint (CMP) approximation. When the velocities used in migration are not the actual velocities of the media, the images of reflectors move away both horizontally and vertically from their actual position. Therefore, the scanning with residual prestack migration that utilizes the common-depth-point (CDP) concept is more appropriate for determining residual velocity (Etgen, 1990; Zhang, 1990). Residual velocity, the measure of residual moveout, is a function of the interval velocity model. The residual velocity that best stacks the image of a reflector is related to the interval velocity model by a filtered

[1] **email:** jun@sep.stanford.edu

traveltime-tomography operator (Etgen, 1990). To convert the residual-velocity information to an updated interval-velocity model, we invert the filtered traveltime tomography operator in one dimension (Al-Yahya, 1987) or two dimensions (Etgen, 1990). Because the interval velocity is found from measured residual velocity by an inversion algorithm, the determination of the residual velocity is very important. Typically the residual velocity is found by manual or automatic picking in a semblance panel obtained by scanning in CRP gathers with a range of residual velocity. Therefore, the measured residual velocity is more reliable if we have better resolution CRP gathers. Since wavefront synthesis imaging produces a clearer image as we increase the number of depths where a plane wave is synthesized, we can have clearer CRP gathers. The CRP gather obtained by wavefront synthesis imaging, however, is somewhat different from those obtained by the other prestack imaging methods. In the next two sections, I explain how to obtain CRP gathers by wavefront synthesis imaging and then describe a method of residual velocity scanning in the CRP gathers.

CRP GATHERS IN WAVEFRONT SYNTHESIS IMAGING

In a multifold seismic experiment, a small portion of a subsurface is illuminated by shots at different offsets (Figure 1). The reflected energy is recorded by a receiver array on the surface. Imaging of such seismic reflection data can be accomplished by a prestack depth migration of individual shot records or common-offset records. The images after migration at a constant surface location comprise a CRP gather (Figure 2); each trace in the CRP gather corresponds to an image obtained from a different source location. If we assume impulses as sources, reflections obtained from different sources correspond to different illumination angles for the same reflector. In order to simulate exactly a CRP gather obtained by shot profile imaging with wavefront synthesis imaging, we would need to synthesize a wavefront for each depth point with an incidence angle determined by the geometry and velocity model between the source location and the reflector. This method would not be efficient because it would require a huge amount of computing time. However, if we recall that, when imaged correctly the image of the subsurface under a surface location should be at the same depth regardless of the source position or the shape of source wavefield, we can define a CRP gather as an image gather of different incidence angles instead of different source locations. Therefore, using wavefront synthesis imaging, we can obtain a CRP gather by synthesizing several plane waves at the surface. This approach will produce a CRP gather with the same quality as that produced by shot-profile imaging. In order to get better quality CRP gathers, we need to simulate plane waves in every depth level. If we assume that a wavefront keeps its shape over a short range of depths, we can generate a common-incidence angle section by synthesizing plane waves for several depth levels. Therefore, the resulting CRP gather (Figure 2) is equivalent to a CRP gather obtained by wavefront synthesis imaging with different illumination angles (Figure 3) in terms of the velocity analysis principle. To illustrate how to generate a CRP gather by wavefront synthesis imaging, I have used a synthetic prestack dataset (Figure 4). This dataset was generated using the finite-difference method with the acoustic velocity model shown in Figure 5. Figure 7 shows a CRP gather (4000 meters at the surface) obtained from 31 planewave syntheses whose angle varies from -30 to 30 degrees at the surface. In

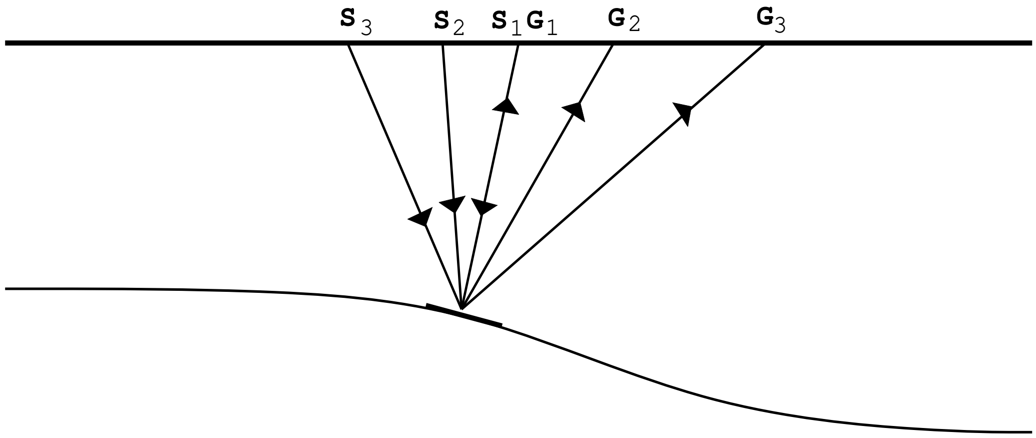

Figure 1: In a multifold seismic experiment, a small portion of the subsurface is illuminated by shots at different offsets with different angles. jun2-crp-ray [NR]

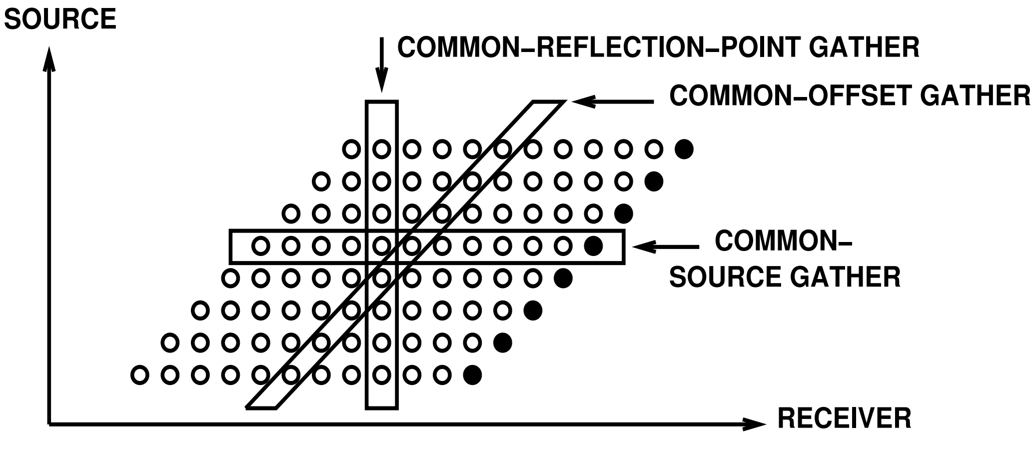

Figure 2: A stacking chart showing a CRP gather after prestack migration. Migration is applied for each common-source gather in profile imaging or for each common-offset gather in constant-offset migration. The solid dots indicate the shots, and the empty dots indicate receivers. jun2-crp1 [NR]

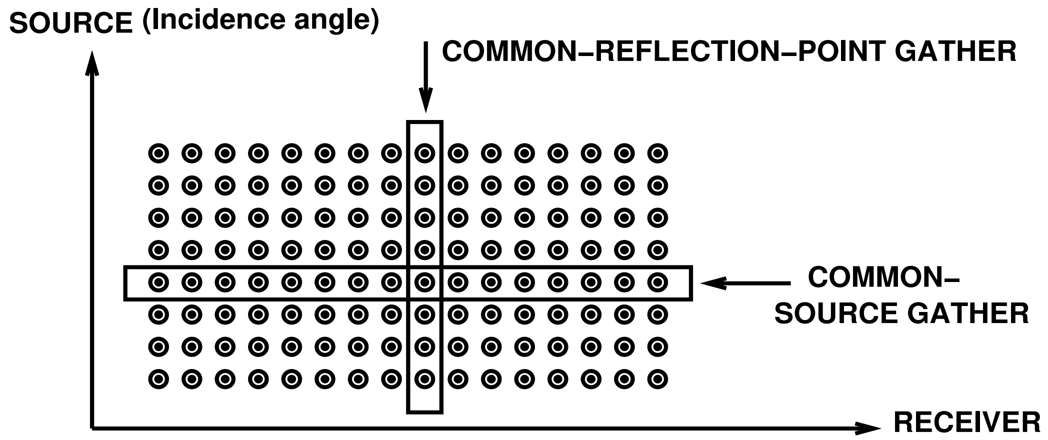

Figure 3: A stacking chart showing a CRP gather after planewave synthesis imaging. Migration is applied for each common-source gather. The small solid dots indicate the shots, and the large empty dots indicate receivers. jun2-crp2 [NR]

Figure 7a, the synthetic dataset has been migrated with the velocity of the medium; in Figure 7b, with a possible initial velocity model of 1-D velocity that increases vertically, as shown in Figure 6. Clearly, the velocity used in Figure 7b is wrong because the resulting image does not have the expected flat horizontal reflection image alignment like that in Figure 7a. Since the CRP gathers provide the main information about velocity of the medium, the clearer the images in CRP gathers, the better. In Figure 7, the reflector images at greater depths are less clear than the images at shallow depths. This is mainly because of the wavefront distortion after extrapolating through the complicated velocity model. In order to obtain clearer images at greater depth, we need to synthesize plane waves not only at the surface but also in the subsurface. Figure 8 shows a CRP gather obtained from 31 planewave syntheses at 15 equi-spaced depth levels. Comparison with Figure 7 shows that Figure 8 provides clearer images at deeper levels. The difference between Figure 7 and Figure 8 becomes apparent when we look at the residual velocity semblance panel in Figures 10 and 11, which are explained in the next section. We are therefore able to make a qualitative comparison between CRP gathers to determine which was migrated with a velocity closest to that of the medium. From the type of curvature (upward or downward), we can also tell whether the velocity used in migration is higher or lower than the velocity of the medium.

SCANNING RESIDUAL VELOCITY

The preceding section shows that by examining CRP gathers we can tell whether the velocity used in migration is correct. In this section, I estimate the error in the average slowness after migration with a preliminary velocity model. To update the velocity model after migration, we need a way of quantifying the deviation of the images in a CRP gather from horizontal alignment. For example, suppose we want to estimate how much to change the velocity used in Figure 7b so that it looks like Figure 7a. We should, therefore, study what happens if we

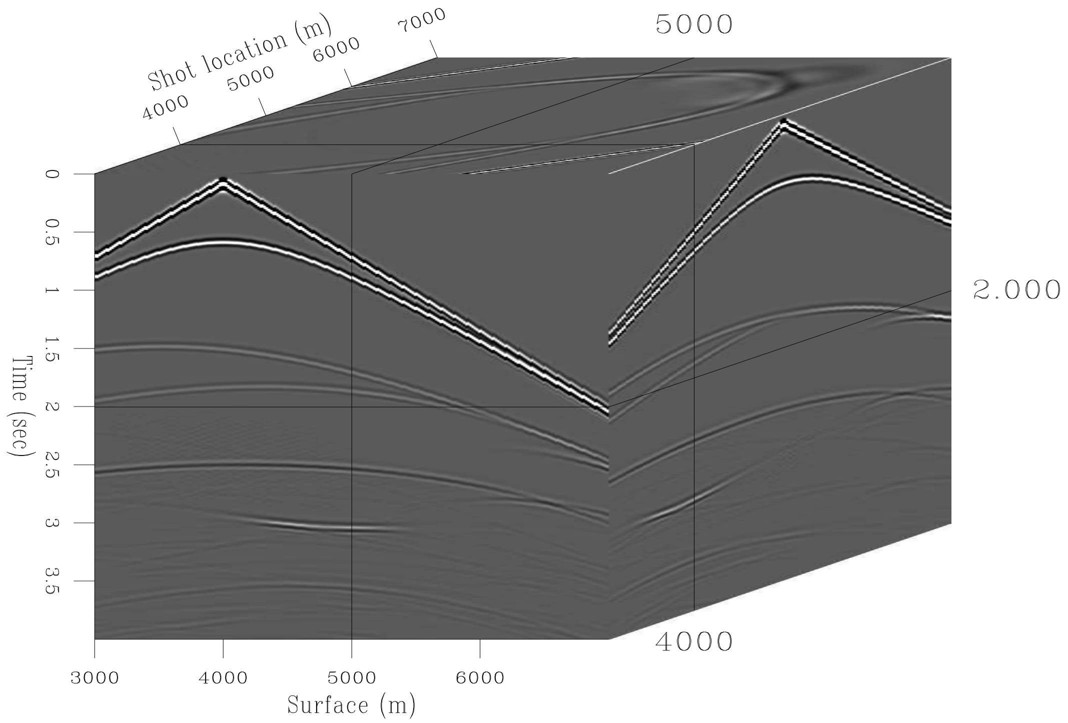

Figure 4: The synthetic dataset for the velocity model shown in Figure 5. jun2-syn-dataset [NR]

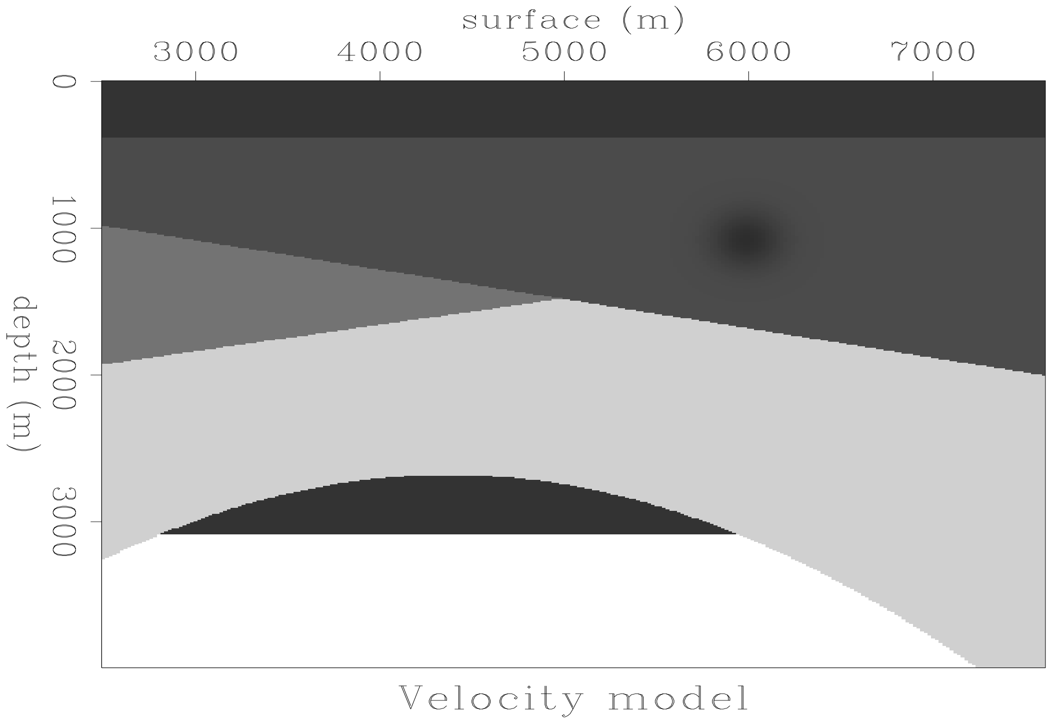

Figure 5: The acoustic velocity model used to generate the synthetic dataset shown in Figure 4. jun2-syn-velocity [ER]

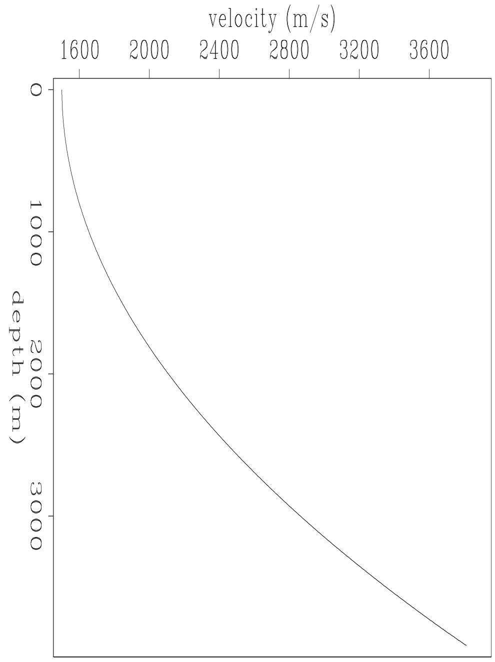

Figure 6: The first trial velocity that increases with depth. jun2-syn-vel-iter0 [ER]

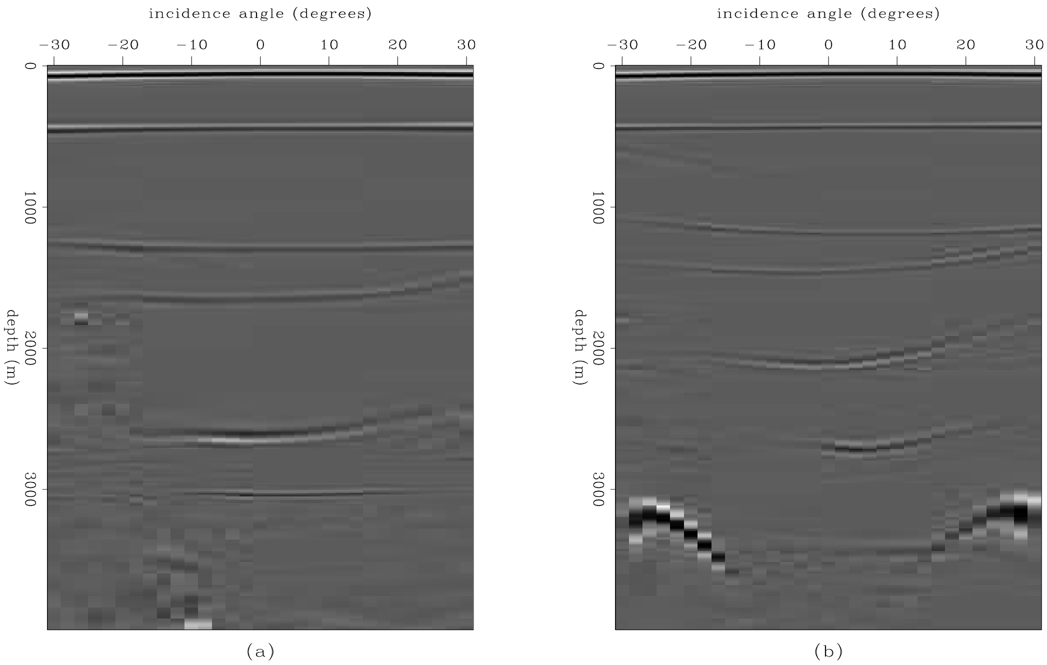

Figure 7: CRP gathers taken from a migrated section by synthesizing a plane wave at the surface (a) with the correct velocity and (b) with the trial velocity. jun2-syn-crp [ER]

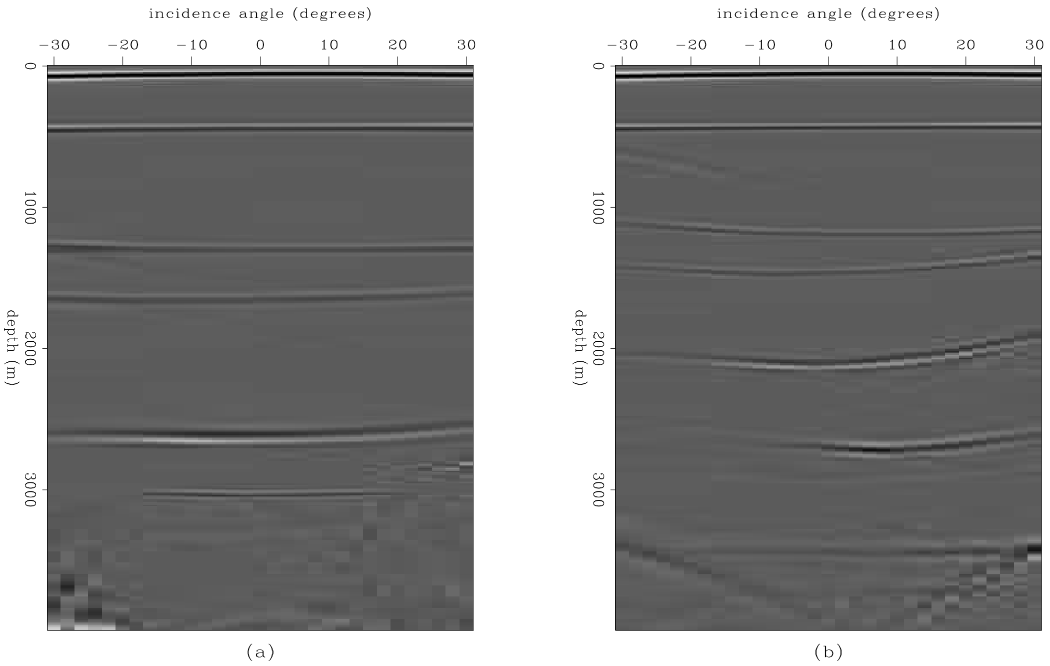

Figure 8: CRP gathers taken from a migrated section by synthesizing plane waves at 15 equispaced depths (a) with the correct velocity and (b) with the trial velocity. jun2-syn-crp-good [ER]

migrate the data using a velocity that is different from that of the medium. Since, as discussed in the preceding section, the curvatures in a post-migration CRP gather are affected by the error in average slowness, I first obtain average slownesses, and then return to interval slownesses.

Horizontal reflector

This section discusses the case of a horizontal reflector, as shown in Figure 9. Let the depth to the reflector be z, the average slowness of the medium to the reflector be $\bar{s}$, and the recorded traveltime t. If a planewave source has incidence angle θ at the reflector, the ray path from and to the reflector will be a straight line and the half offset x of the ray path can be calculated from the incidence angle θ of the planewave and the reflector depth z, as follows:

$$x = z\tan\theta. \tag{1}$$

Then the traveltime is given by

$$t = 2\sqrt{x^2+z^2}\cdot\bar{s}. \tag{2}$$

After migration with the slowness of the medium, the image under a surface location will be at same depth z. If we migrate with an average slowness $\bar{s}_m$ instead of with the slowness of the medium itself, the image under a surface location will be at depth z_m. In this case, the traveltime is given by

$$t = 2\sqrt{x^2+z_m^2}\cdot\bar{s}_m. \tag{3}$$

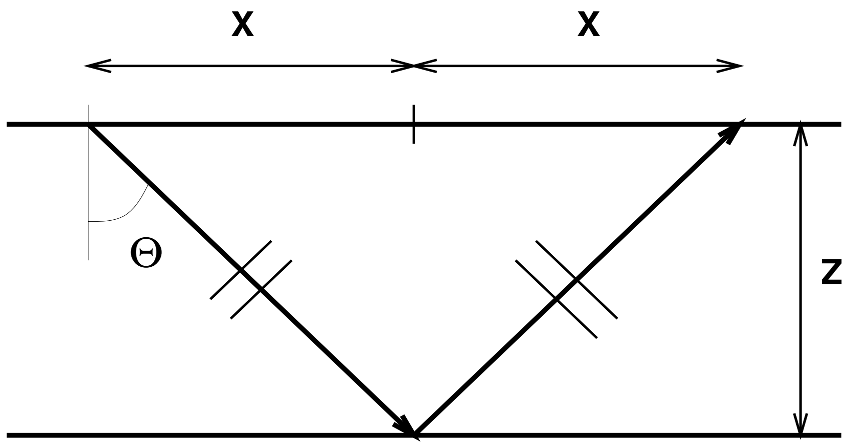

Figure 9: Ray travel path of a plane wave for a flat reflector. jun2-raypath-flat [NR]

The traveltime, t, is the same in equations (2) and (3) because it is an observed quantity. The ambiguity occurs between slowness and depth. Eliminating t from equations (2) and (3), we obtain

$$z_m = \sqrt{\gamma^2 z^2 + (\gamma^2 - 1)x^2}, \tag{4}$$

where

$$\gamma = \frac{\bar{s}}{\bar{s}_m}. \tag{5}$$

Equation (4) gives a relation between the apparent depth, z_m, and the actual depth, z; they are linked through the parameter γ. Note that they are equal regardless of the offset or the incidence angle of the plane wave, when the slowness used in migration is equal to the slowness of the medium ($\gamma = 1$). When γ is not equal to 1, both a moveout as a function of offset and a shift at zero offset occur. At zero offset ($x = 0$), there is the well-known ambiguity between depth and velocity,

$$z_m = \gamma z, \tag{6}$$

or

$$z_m \bar{s}_m = z \bar{s}. \tag{7}$$

In equation (7), we know the values of $\bar{s}_m$ (from the migration slowness that we used) and z_m (the depth given by migration with slowness $\bar{s}_m$). We cannot determine both z (the actual depth) and $\bar{s}$ (the actual slowness), because many combinations of these two quantities may satisfy the relation expressed in equation (7). This argument explains why velocity analysis cannot be done by synthesizing one plane wave, just as it cannot be done by zero-offset migration. The curvature in a CRP gather will vary from depth to depth, depending on the velocity error at each depth. Therefore, the parameter γ is not a constant for a CRP gather but rather a function of depth, $\gamma(z)$. For instance, all the events in the CRP gather of Figure 7b are curved upward; the slowness used in migration is high for all depths. The curvature (or lack of it) in the CRP gather can therefore be used to estimate the error (or lack of it) in the velocity model. What we need now is a way to measure curvature. In this example, I measure curvature by searching. At each depth, a curvature is defined by the parameter γ in equation (4). The data are then summed along this curved trajectory. The summation is done for a range of γ, and the sum is biggest for that value of γ that matches the curvature. Because some signals may be weaker than others, the sum is normalized. This normalized summation is similar to the normalized summation commonly known as semblance that is obtained along a hyperbola using the NMO equation (Taner and Koehler, 1969). If the data in a CRP gather are $p(z_m, \theta)$, then searching for curvature produces the semblance panel

$$g(z_m, \gamma) = \frac{[\sum_\theta p(z_m = \sqrt{z_m^2 + (\gamma^2 - 1) z_m^2 \tan^2 \theta}, \theta)]^2}{\sum_\theta [p(z_m = \sqrt{z_m^2 + (\gamma^2 - 1) z_m^2 \tan^2 \theta}, \theta)]^2}. \quad (8)$$

Equation (8) transforms the migrated panel $p(z_m, \theta)$ to the residual velocity panel $g(z_m, \gamma)$. Figures 10 and 11 show the results of that transformation. In these figures, we can notice that the trial velocity is slower than the actual velocity because most of high semblance values appear in the region $\gamma < 1$. Figure 10 shows semblance panels for the CRP gathers obtained by synthesizing plane waves only at the surface (Figures 7) and Figure 11 shows semblance panels for the CRP gathers obtained by synthesizing plane waves not only at the surface but also in the subsurface (Figures 8). Comparing Figures 7and 8, we see quite an improvement in the resolution of the semblance panel when we used plane wave synthesis both at the surface and at the subsurface in either correct or wrong velocity.

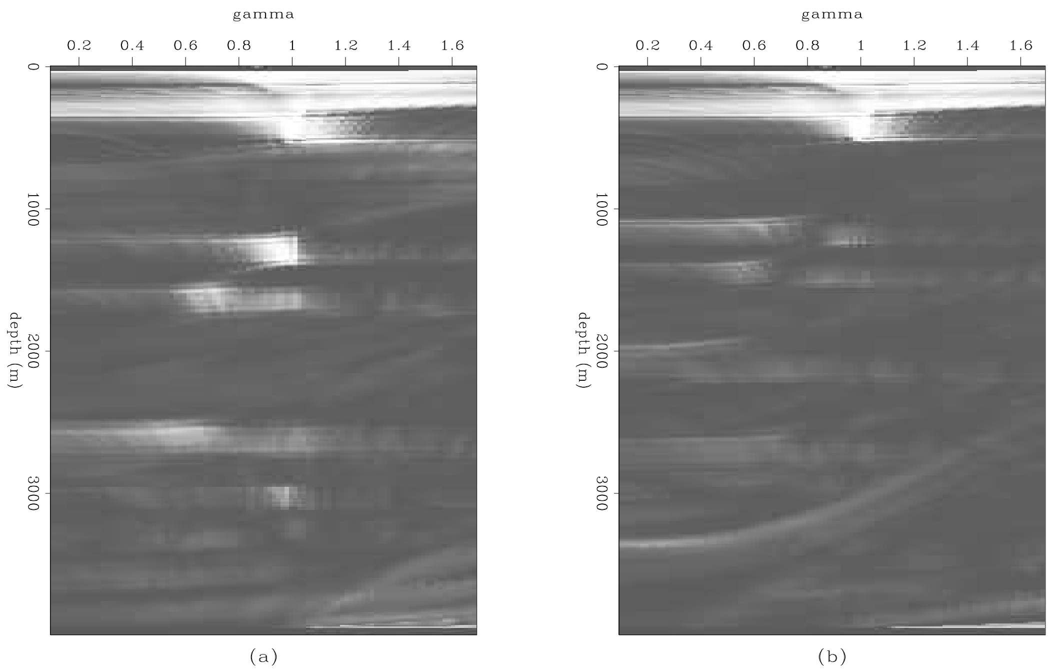

Figure 10: Semblance panels for the CRP gathers shown in Figure 7. jun2-syn-gam-sem [ER]

CONCLUSIONS

The CRP gathers in wavefront synthesizing imaging are generated by synthesizing several plane waves with different incidence angles. By increasing the number of depths for synthe-

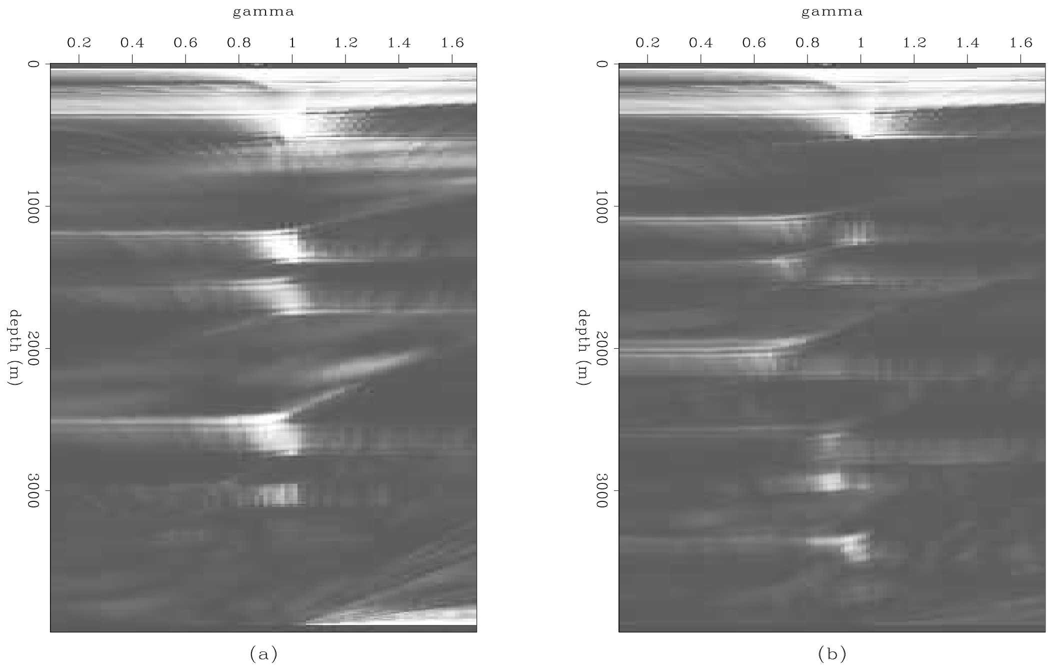

Figure 11: Semblance panels for the CRP gathers shown in Figure 8. jun2-syn-gam-sem-good [ER]

sizing, we can obtain higher-resolution CRP gathers. The residual moveout curve in a CRP gather is defined in terms of incidence angles instead of offsets. Residual velocity analysis in these CRP gathers can be done by scanning over a range of residual velocities in each CRP gather, much as we do in a CRP gather obtained by other prestack migrations. In order to increase the resolution of the residual velocity panel, we need to use the dip-dependent moveout curve.

REFERENCES

Al-Yahya, K. M., 1987, Velocity analysis by iterative profile migration: Ph.D. Thesis, Stanford University.

Berkhout, A. J., 1992, Areal shot record technology: Journal of Seismic Exploration, **1**, 251–264.

Claerbout, J. F., 1985, Imaging the Earth's Interior: Blackwell Scientific Publications.

Etgen, J. T., 1990, Residual prestack migration and interval-velocity estimation: Ph.D. Thesis, Stanford University.

Ji, J., 1993, Controlled illumination by wavefront synthesis: SEP–**79**, 129–144.

Rietveld, W. E. A., Berkhout, A. J., and Wapenaar, C. P. A., 1992, Optimum seismic illumination of hydrocarbon reservoirs: Geophysics, **57**, 1334–1345.

Rietveld, W. E. A. and Berkhout, A. J., 1992, Depth migration combined with controlled illumination: 62th Ann. Internat. Mtg., Soc. Expl. Geophys., Expanded Abstracts, 931–934.

Schultz, P. S. and Claerbout, J. F., 1978, Velocity estimation and downward continuation by wavefront synthesis: Geophysics, **43**, 691–714.

Zhang, L., 1990, Refining the image of profile migration: residual moveout and residual migration: SEP–**65**, 29–40.